




# CD73 contributes to the pathogenesis of fusion-negative rhabdomyosarcoma through the purinergic signaling pathway

Karla Cano Hernandez<sup>a,b</sup>, Akansha M. Shah<sup>a,b</sup>, Victor A. Lopez<sup>a</sup>, Vincent S. Tagliabracchi<sup>a,b,c,d</sup>, Kenian Chen<sup>e</sup>, Lin Xu<sup>e</sup>, Rhonda Bassel-Duby<sup>a,b</sup>, Eric N. Olson<sup>a,b,1</sup> , and Ning Liu<sup>a,b,1</sup>

Contributed by Eric N. Olson; received September 18, 2023; accepted November 29, 2023; reviewed by Michael Kyba and Thomas A. Rando

Rhabdomyosarcoma (RMS) is the most common type of soft tissue sarcoma in children and adolescents. Fusion-negative RMS (FN-RMS) accounts for more than 80% of all RMS cases. The long-term event-free survival rate for patients with high-grade FN-RMS is below 30%, highlighting the need for improved therapeutic strategies. CD73 is a 5' ectonucleotidase that hydrolyzes AMP to adenosine and regulates the purinergic signaling pathway. We found that CD73 is elevated in FN-RMS tumors that express high levels of TWIST2. While high expression of CD73 contributes to the pathogenesis of multiple cancers, its role in FN-RMS has not been investigated. We found that CD73 knockdown decreased FN-RMS cell growth while up-regulating the myogenic differentiation program. Moreover, mutation of the catalytic residues of CD73 rendered the protein enzymatically inactive and abolished its ability to stimulate FN-RMS growth. Overexpression of wildtype CD73, but not the catalytically inactive mutant, in CD73 knockdown FN-RMS cells restored their growth capacity. Likewise, treatment with an adenosine receptor  $A_{2A-B}$  agonist partially rescued FN-RMS cell proliferation and bypassed the CD73 knockdown defective growth phenotype. These results demonstrate that the catalytic activity of CD73 contributes to the pathogenic growth of FN-RMS through the activation of the purinergic signaling pathway. Therefore, targeting CD73 and the purinergic signaling pathway represents a potential therapeutic approach for FN-RMS patients.

sarcoma | cell signaling | pediatric cancer | Cell biology

Rhabdomyosarcoma (RMS) is the most common type of soft tissue sarcoma in children and adolescents. RMS arises from the mesodermal lineage and exhibits features of undifferentiated muscle cells (1). However, RMS cells are blocked early in the muscle differentiation pathway and lack expression of terminal myogenic markers even amid high levels of skeletal muscle master regulators such as MyoD (1). RMS is classified into two main types based on their molecular characteristics: fusion-positive RMS (FP-RMS) and fusion-negative RMS (FN-RMS). FP-RMS harbors chromosomal translocations  $t(2;13)$  and  $t(1;13)$  that result in the generation of PAX3-FOXO1 or PAX7-FOXO1 fusion oncoproteins (2). In contrast, FN-RMS, which accounts for more than 80% of all RMS cases, does not carry these chromosomal translocations, and recurrent driver mutations were found to be uncommon (3). Around 15% of all RMS patients present with metastases when diagnosed, and the long-term event-free survival rate for these cases is below 30% (2, 4). Therefore, an improved understanding of the molecular etiology of FN-RMS will inform the development of new therapeutic strategies.

We sought to investigate the molecular mechanisms that drive FN-RMS. Previously, we showed that FN-RMS patient tumors harbor copy number variations of the TWIST2 locus (5). The TWIST2 transcription factor controls the differentiation of mesodermal lineages, such as the skeletal muscle. TWIST2 knockdown in FN-RMS decreases tumor growth while enhancing myogenic differentiation (6). Through ChIP-Sequencing (ChIP-Seq) and RNA-Sequencing (RNA-Seq) analysis, we identified CD73 as a TWIST2 target gene. CD73, also known as NT5E, is a 5' ectonucleotidase that homodimerizes and catalyzes the production of adenosine (7). CD73 works with ectonucleoside triphosphate diphosphohydrolase-1 (ENTPD1), also known as CD39, in the extracellular space. CD39 acts upstream of CD73 by hydrolyzing adenosine triphosphate (ATP) and adenosine diphosphate (ADP) to adenosine monophosphate (AMP), which is then further hydrolyzed to adenosine by CD73 (7). Adenosine in the extracellular space binds adenosine receptors ( $A_1$ ,  $A_{2A}$ ,  $A_{2B}$ , and  $A_3$ ) in the cell membrane and stimulates the purinergic signal transduction pathway modulating cell growth, survival, and differentiation (8).

In the tumor microenvironment, adenosine produced by CD73 suppresses the immune response by preventing activation of neutrophils, T cells, T regulatory cells ( $T_{REG}$ ), dendritic cells (DCs), and natural killer (NK) cells that express adenosine receptors (9, 10).

## Significance

Fusion-negative rhabdomyosarcoma (FN-RMS) accounts for more than 80% of all rhabdomyosarcoma cases. However, the mechanisms driving FN-RMS remain poorly understood, resulting in limited therapeutic strategies. We identified CD73, a cell membrane 5' ectonucleotidase, as a TWIST2 regulated gene contributing to the pathogenesis of FN-RMS. We show that knockdown of CD73 decreased FN-RMS pathogenic growth in vitro and in vivo. Moreover, CD73 knockdown induced cell cycle arrest and decreased migration while initiating the myogenic program in FN-RMS cells. We also showed that the role of CD73 in FN-RMS is mediated by its enzymatic activity and the activation of the purinergic signaling pathway. Our results warrant consideration of CD73 as a potential therapeutic target in FN-RMS.

Author contributions: K.C.H., V.A.L., V.S.T., K.C., R.B.-D., E.N.O., and N.L. designed research; K.C.H., A.M.S., V.A.L., and V.S.T. performed research; K.C.H. analyzed data; K.C. and L.X. analyzed bioinformatic data; and K.C.H., E.N.O., and N.L. wrote the paper.

Reviewers: M.K., University of Minnesota; and T.A.R., University of California Los Angeles.

The authors declare no competing interest.

Copyright © 2024 the Author(s). Published by PNAS. This article is distributed under [Creative Commons Attribution-NonCommercial-NoDerivatives License 4.0 \(CC BY-NC-ND\)](https://creativecommons.org/licenses/by-nc-nd/4.0/).

<sup>1</sup>To whom correspondence may be addressed. Email: Eric. Olson@utsouthwestern.edu or Ning.Liu@utsouthwestern.edu.

This article contains supporting information online at <https://www.pnas.org/lookup/suppl/doi:10.1073/pnas.2315925121/-/DCSupplemental>.

Published January 16, 2024.

Interestingly, a highly immunosuppressed microenvironment is a common feature of multiple types of cancer; thus, targeting CD73 is an appealing option for enhancing antitumor immunity and restoring the therapeutic benefit of immunotherapies (11–14). Moreover, high expression of CD73 also promotes progression, invasion, and metastasis in melanoma and breast cancer (15, 16). These oncogenic functions of CD73 can be reversed by CD73 inhibitors and neutralizing antibodies that are currently being tested in clinical trials (17–20).

Here, we investigated the cell-autonomous role of CD73 in FN-RMS progression in vitro and in vivo. We show that CD73 knockdown in FN-RMS cells significantly decreases cell proliferation and migration while inducing the myogenic differentiation program. Additionally, CD73 knockdown reduces tumor growth in xenograft models. We generated a catalytically inactive CD73 mutant that failed to rescue the CD73 knockdown growth defect, indicating that CD73 functions via its enzymatic activity in FN-RMS. In line with these findings, an adenosine receptor  $A_{2A-B}$  agonist was able to partially reverse the effects of CD73 knockdown. Overall, these results suggest that CD73 contributes to the pathogenic growth of FN-RMS through the purinergic signaling pathway.

## Results

**CD73 Regulates Proliferation of FN-RMS Cells.** We showed previously that loss of function of the TWIST2 transcription factor in FN-RMS cells decreases their oncogenic potential in vitro and in vivo, resulting in a global shift in gene expression toward a postmitotic, differentiated skeletal muscle cell type (6). With the aim of finding potential druggable targets for FN-RMS, we sought to identify TWIST2 regulated genes that dictate the oncogenic capacity of FN-RMS. RNA-seq analysis revealed ~1,000 genes that were differentially expressed in TWIST2-knockdown xenograft tumors (6). Among these genes, CD73 was substantially downregulated upon TWIST2 knockdown (Fig. 1*A*). TWIST2 ChIP-Seq in RD cells, a patient-derived FN-RMS cell line, revealed binding sites for TWIST2 at the CD73 locus that overlapped with H3K27ac peaks, indicative of an open, transcriptionally active enhancer region (Fig. 1*B*) (6). These findings suggest that the CD73 gene is a direct transcriptional target of TWIST2. To further confirm that TWIST2 regulates CD73 expression, we evaluated CD73 protein levels in RD cells upon TWIST2 overexpression and knockdown by western blot (6). Expression of CD73 was increased when TWIST2 was overexpressed and decreased when TWIST2 was knocked down (Fig. 1*C*). We investigated CD73 expression in different FN-RMS (RD and JR-1) and FP-RMS (RH30 and RH4) cell lines. Western blot analysis showed that CD73 is highly expressed in FN-RMS cells compared to FP-RMS cells (Fig. 1*D*). In addition to RD and JR-1 cells, CD73 was expressed in the SMS-CTR and RH18 FN-RMS cell lines (SI Appendix, Fig. S1*A*).

To begin to elucidate the role of CD73 in FN-RMS, we used two different shRNAs (sh1-CD73 and sh2-CD73) targeting the 3'UTR of the mRNA to knockdown CD73 in RD and JR-1 cells. A nontargeting scrambled shRNA (shScr) was used as the control. Compared to shScr, we observed a decrease in CD73 mRNA and protein expression in RD (SI Appendix, Fig. S1*B* and *C*) and JR-1 cells (SI Appendix, Fig. S1*D* and *E*) upon CD73 shRNA knockdown. We then performed EdU labeling to examine the effect of CD73 knockdown on cell growth and found a decrease in EdU incorporation when CD73 was knocked down in these cells (Fig. 1*E–G*). These findings suggest that CD73 promotes FN-RMS cell proliferation.

## CD73 Knockdown Reduces FN-RMS Oncogenic Potential In Vitro.

To further study the function of CD73 in FN-RMS pathogenesis, we generated a stable RD cell line with doxycycline (Dox)-inducible shRNA targeting CD73 (ish-CD73) (Fig. 2*A*). qRT-PCR and Western blot analysis confirmed efficient knockdown of CD73 mRNA and protein in ish-CD73 cells after 48 h of Dox treatment (CD73<sup>KD</sup>) compared to No-Dox ish-CD73 RD cells (Control) (SI Appendix, Fig. S2*A* and *B*). EdU labeling revealed a decrease in ish-CD73 cell proliferation in CD73<sup>KD</sup> compared to control cells (Fig. 2*B* and *C*), similar to our previous transient shRNA infection results (Fig. 1*E* and *F*). To control for the effect of Dox treatment, we generated a Dox inducible scrambled shRNA cell line (ish-Scr). There was no difference in EdU incorporation in the ish-Scr RD cells upon Dox treatment (SI Appendix, Fig. S2*C* and *D*), indicating that Dox itself does not affect cell proliferation. Hereafter, we used the Dox-inducible ish-CD73 stable RD cell line to investigate the role of CD73 in FN-RMS.

We determined whether CD73 knockdown in RD cells affected cell cycle progression, using DAPI staining and flow cytometry to assess DNA content. Knockdown of CD73 in RD cells resulted in an increase in the percent of cells in the G0-G1 phase with fewer cells in the S and G2-M phases compared to control cells (Fig. 2*D* and SI Appendix, Fig. S2*E*). These results suggest that CD73 knockdown induces cell cycle arrest in the G0-G1 phase in RD cells. To determine whether CD73 knockdown influenced the clonogenic potential of RD cells, we performed colony formation assays in CD73<sup>KD</sup> and control cells and found a reduction in colony forming capacity upon CD73 knockdown (Fig. 2*E* and *F*). We further determined that this growth defect was not a result of increased cell death by staining CD73<sup>KD</sup> and control cells with Annexin-V and propidium iodide followed by flow cytometry analysis (SI Appendix, Fig. S2*F*). In addition, Cleaved Caspase-3 protein levels were slightly decreased in CD73<sup>KD</sup>, confirming the lack of apoptotic cell death (SI Appendix, Fig. S2*G*). Since elevated expression of CD73 has been suggested to promote a migratory phenotype in different types of cancers, we investigated the effect of CD73 knockdown on the migration potential of RD cells using a transwell migration assay (Fig. 2*G*) (8, 16). CD73<sup>KD</sup> RD cells displayed a reduced migratory capacity compared to control cells (Fig. 2*H* and *I*). Consistent with these findings, western blot analysis showed that CD73<sup>KD</sup> RD cells resulted in decreased expression of proteins involved in migration, such as N-Cadherin (N-CAD), AXL receptor tyrosine kinase (AXL), and L1 cell adhesion molecule (L1CAM) (Fig. 2*J*). Altogether, our findings demonstrate that CD73 knockdown induces cell cycle arrest and reduces the clonogenic and migratory potential of RD cells.

## Knockdown of CD73 Decreases Tumor Growth in Xenografts.

To elucidate the role of CD73 in tumor growth in vivo, we performed xenograft experiments using ish-CD73 RD cells. To monitor tumor growth in vivo using bioluminescence imaging, we infected ish-CD73 RD cells with lentivirus expressing a luciferase reporter (ish-CD73-luc) (Fig. 3*A*). We treated ish-CD73-luc RD cells with Dox for 96 h to induce CD73 knockdown before injecting  $7 \times 10^6$  cells into the flank of nonobese diabetic severe combined immunodeficient (NOD-SCID) mice. No-Dox ish-CD73-luc RD cells served as control. Prior to injection, we confirmed that CD73 protein expression was reduced in the Dox-treated group (CD73<sup>KD</sup>-luc) compared to the No-Dox group (Control) (Fig. 3*B*). Imaging and quantification of the luciferase signal over 4 wk demonstrated a substantial reduction in luciferase signal upon CD73 knockdown (Fig. 3*C–E*). We harvested the tumors four weeks after injection and observed that CD73<sup>KD</sup>-luc tumors were smaller in size and reduced in

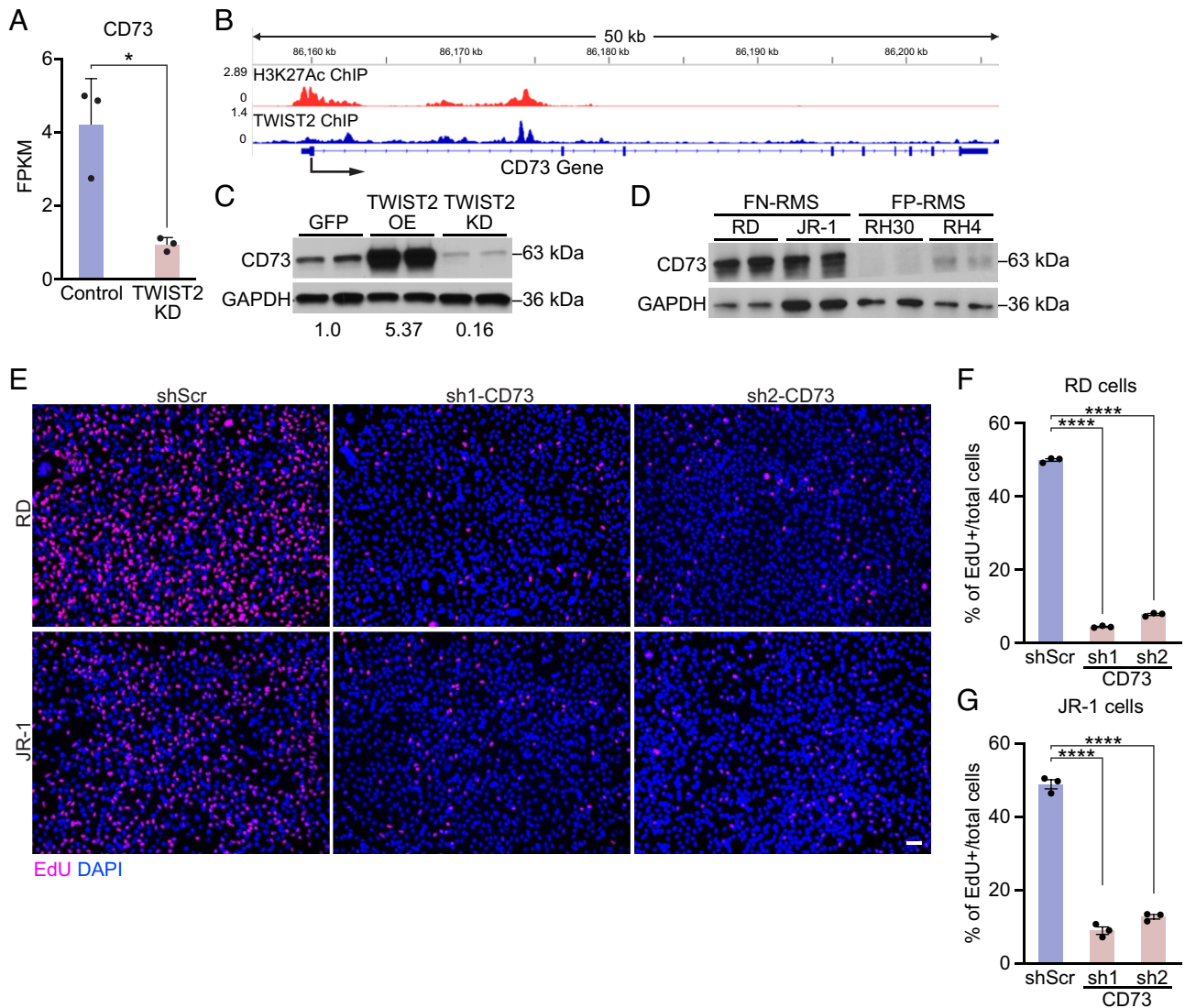


**Fig. 1.** CD73, a TWIST2-target gene, regulates proliferation of FN-RMS cell lines. (A) CD73 mRNA expression in TWIST2 knockdown (KD) and control FN-RMS xenografts as determined by RNA-seq. Values for Fragments Per Kilobase per Million (FPKM) mapped fragments are shown.  $n = 3$  independent experiments  $*P < 0.05$ . Data are shown as mean  $\pm$  SEM; Student's  $t$  test two-tailed. (B) TWIST2 ChIP-seq shows TWIST2 binding peaks (blue) at the CD73 locus correlated with H3K27ac ChIP-seq peaks (red) in RD cells. (C) Western blot showing protein levels of CD73 in RD cells infected with lentivirus encoding GFP, TWIST2 (TWIST2 OE), and a shRNA targeting TWIST2 (TWIST2 KD). GAPDH is the loading control. *Bottom*: Average densitometry ratios of TWIST2 OE/GFP and TWIST2 KD/GFP. (D) Western blot showing CD73 protein levels in the FN-RMS and FP-RMS cell lines. GAPDH is the loading control. (E) EdU staining (magenta) upon EdU pulse in RD (*Top*) and JR-1 (*Bottom*) cell lines upon CD73 knockdown with two different shRNAs (sh1-CD73 and sh2-CD73) compared to shScr control. Nuclei were stained with DAPI (blue). (Scale bar, 50  $\mu\text{m}$ .) (F and G) Quantification of EdU+ cells over the total number of cells in RD (F) and JR-1 (G);  $n = 3$  independent experiments  $****P < 0.0001$ , results are shown as mean  $\pm$  SEM; two-way ANOVA test.

weight compared to control tumors (Fig. 3 F and G). Moreover, hematoxylin and eosin (H&E) staining indicated a lower cell density in CD73<sup>KD</sup>-luc tumors (Fig. 3H). We also found a reduction in the number of cycling cells in CD73<sup>KD</sup>-luc tumors compared to control by immunostaining for Ki67 (Fig. 3 H and I). These results suggest that CD73 contributes to tumor growth in FN-RMS xenograft models.

**CD73 Knockdown Decreases Oncogenic Gene Expression while Enhancing Myogenesis.** To examine the transcriptional influence of CD73, we performed RNA-seq on CD73<sup>KD</sup> and No-Dox control ish-CD73 RD cells (Fig. 4 A and B). RNA-seq analysis revealed that greater than 1,400 genes were down-regulated upon CD73 knockdown. These genes were associated with gene ontology (GO) terms related to regulation of cell adhesion, response to growth factor, and extracellular matrix organization (Fig. 4 C, *Bottom*).

Interestingly, the PI3K-AKT signaling pathway was one of the most down-regulated pathways in CD73<sup>KD</sup> RD cells. The serine/threonine kinase AKT regulates cell proliferation and contributes to cancer pathogenesis by phosphorylating and activating downstream effector molecules (21, 22). We evaluated whether CD73 knockdown in RD cells influenced levels of Akt phosphorylation. While total AKT levels did not change in CD73<sup>KD</sup>, phosphorylated AKT (pAKT) was reduced (Fig. 4D). We also analyzed the activity of other oncogenic signaling molecules such as MEK, JUN, and MYC, and observed decreased expression of these proteins upon CD73 knockdown (Fig. 4E). Phosphorylated and activated forms of the JUN and MEK proteins were also reduced in CD73<sup>KD</sup> cells (Fig. 4E), indicating an overall decrease in oncogenic signaling with CD73 loss.

A hallmark of FN-RMS cells is the lack of myogenic differentiation despite expression of master regulators of myogenesis such as

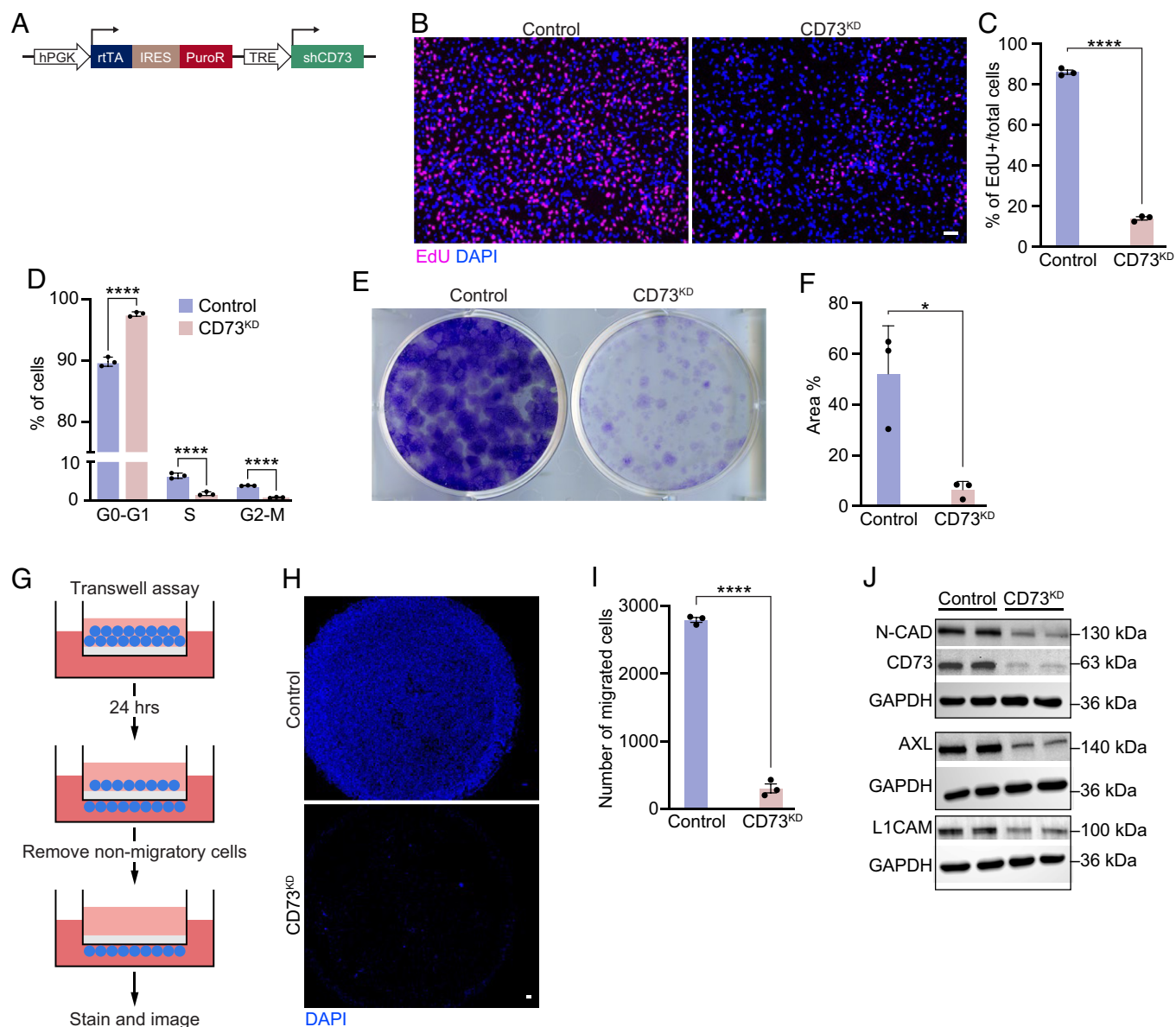


**Fig. 2.** CD73 knockdown reduces growth and migration of RD cells. (A) Schematic depicting the Dox-inducible CD73 knockdown construct consisting of human phosphoglycerate kinase (hPGK) promoter, reverse tetracycline-controlled transactivator (rtTA), internal ribosome entry sites (IRES), puromycin resistance (PuroR), and tetracycline response element (TRE) followed by the shRNA targeting CD73. CD73<sup>KD</sup> is achieved by 48 to 96 h of Dox treatment in RD cells. No-Dox ish-CD73 RD cells served as control. (B) EdU staining (magenta) in CD73<sup>KD</sup> RD cells compared to No-Dox ish-CD73 control RD cells. Nuclei were stained with DAPI (blue). (Scale bar, 50  $\mu$ m.) (C) Quantification of EdU+ cells over the total number of cells in B; n = 3 independent experiments \*\*\*\*P < 0.0001, results are shown as mean  $\pm$  SEM; Student's *t* test two-tailed. (D) Quantification of the percentage of CD73<sup>KD</sup> RD cells and No-Dox ish-CD73 control RD cells in the G0-G1, S, and G2-M stages of the cell cycle as determined by flow cytometry for DNA content; n = 3 independent experiments \*\*\*\*P < 0.0001, results are shown as mean  $\pm$  SEM; two-way ANOVA test. (E) Crystal violet staining of colony formation assay in CD73<sup>KD</sup> RD cells compared to No-Dox ish-CD73 control RD cells. (F) Quantification of the percent area of colony coverage in E; n = 3 independent experiments \*P < 0.05, results are shown as mean  $\pm$  SEM; Student's *t* test two-tailed. (G) Schematic of the transwell migration assay. (H) DAPI immunostaining (blue) of the bottom face of transwell migration chamber for CD73<sup>KD</sup> RD cells compared to No-Dox ish-CD73 control RD cells. (Scale bar, 50  $\mu$ m.) (I) Quantification of the total number of cells that migrated to the bottom face of the transwell migration chamber in H; n = 3 independent experiments \*\*\*\*P < 0.0001, results are shown as mean  $\pm$  SEM; Student's *t* test two-tailed. (J) Western blot analysis of CD73<sup>KD</sup> RD cells compared to No-Dox ish-CD73 control RD cells, showing protein levels of N-CAD, AXL, and L1CAM expression. GAPDH is the control for total protein.

MYOD (1). Interestingly, 1,083 genes with GO terms related to myogenesis, muscle system process, muscle structure development, and myotube differentiation were up-regulated in CD73<sup>KD</sup> RD cells (Fig. 4 C, *Top*). This suggests that the downregulation of CD73 can drive FN-RMS cells toward myogenic differentiation. To examine this effect further, we subjected CD73<sup>KD</sup> and control RD cells to muscle differentiation media for 6 d. We then assessed the expression of myosin heavy chain (MHC), a marker of terminal myogenic differentiation by immunostaining, which revealed positive MHC staining in CD73<sup>KD</sup> RD cells (Fig. 4 F and G). Moreover, the expression of proteins related to myogenic differentiation such as

MYOD, MEF2C, MYOMAKER, and MYOGENIN was also increased in CD73<sup>KD</sup> RD cells (Fig. 4H). Additionally, we assessed the effect of CD73 knockdown on myogenic differentiation using JR-1 cells. We infected JR-1 cells with sh1-CD73 or shScr as control and then subjected the cells to 6 d of myogenic differentiation. Similar to RD cells, upon CD73 knockdown, JR-1 cells showed positive MHC staining (*SI Appendix, Fig. S3 A and B*) and increased MEF2C protein expression (*SI Appendix, Fig. S3 C*). Altogether, our findings suggest that CD73 knockdown in RD cells reduces the expression of oncogenic genes and promotes the expression of genes involved in terminal myogenesis.

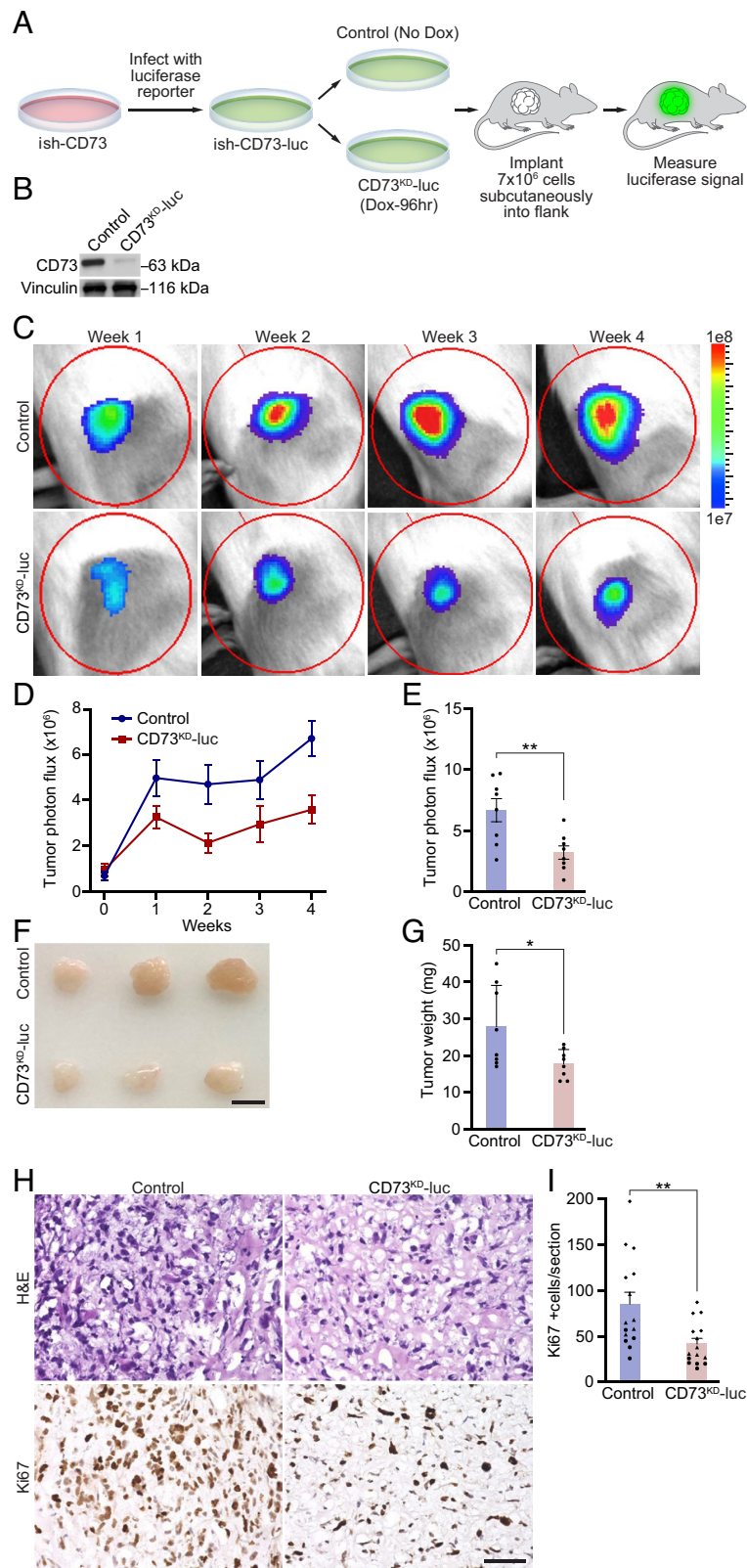


**Fig. 3.** Knockdown of CD73 reduces tumor growth in xenograft models. (A) Diagram illustrating the generation of the ish-CD73-luc RD cell line and xenograft model. CD73<sup>KD</sup>-luc was achieved after 96 h of Dox treatment. No-Dox ish-CD73-luc RD cells were used as control. (B) Western blot analysis of CD73 protein expression in CD73<sup>KD</sup>-luc RD cells compared to No-Dox ish-CD73-luc control RD cells. Vinculin is the control for total protein. (C) Weekly luciferase imaging after xenograft of CD73<sup>KD</sup>-luc RD cells compared to No-Dox ish-CD73-luc control RD cells. (D) Quantification of xenograft tumor luciferase imaging (tumor photon flux) over 4 wk in mice injected with CD73<sup>KD</sup> RD cells compared to No-Dox ish-CD73-luc control RD cells; control (n = 8) and CD73<sup>KD</sup> (n = 8) mice. (E) Week four xenograft luciferase signal quantification (Tumor photon flux) in mice injected with CD73<sup>KD</sup> RD cells compared to No-Dox ish-CD73-luc control RD cells; control (n = 8) and CD73<sup>KD</sup> (n = 8) mice **\*\*P** < 0.01, results are shown as mean ± SEM; Student's *t* test two-tailed. (F) Tumor images and (G) tumor weights at four weeks after xenograft of CD73<sup>KD</sup> RD cells compared to No-Dox ish-CD73-luc control RD cells; control (n = 8) and CD73<sup>KD</sup> (n = 8) mice **\*P** < 0.05, results are shown as mean ± SEM; Student's *t* test two-tailed. (Scale bar, 1 cm.) (H) H&E (Top) and immunohistochemistry staining of Ki67 (Bottom) of tumor sections 4 wk after xenograft of CD73<sup>KD</sup> RD cells compared to No-Dox ish-CD73-luc control RD cells. (Scale bar, 50 μm.) (I) Quantification of Ki67-positive cells per section in H; control (n = 3) and knockdown (n = 3) mice, five images were quantified per mouse. **\*\*P** < 0.01, results are shown as mean ± SEM; Student's *t* test two-tailed.

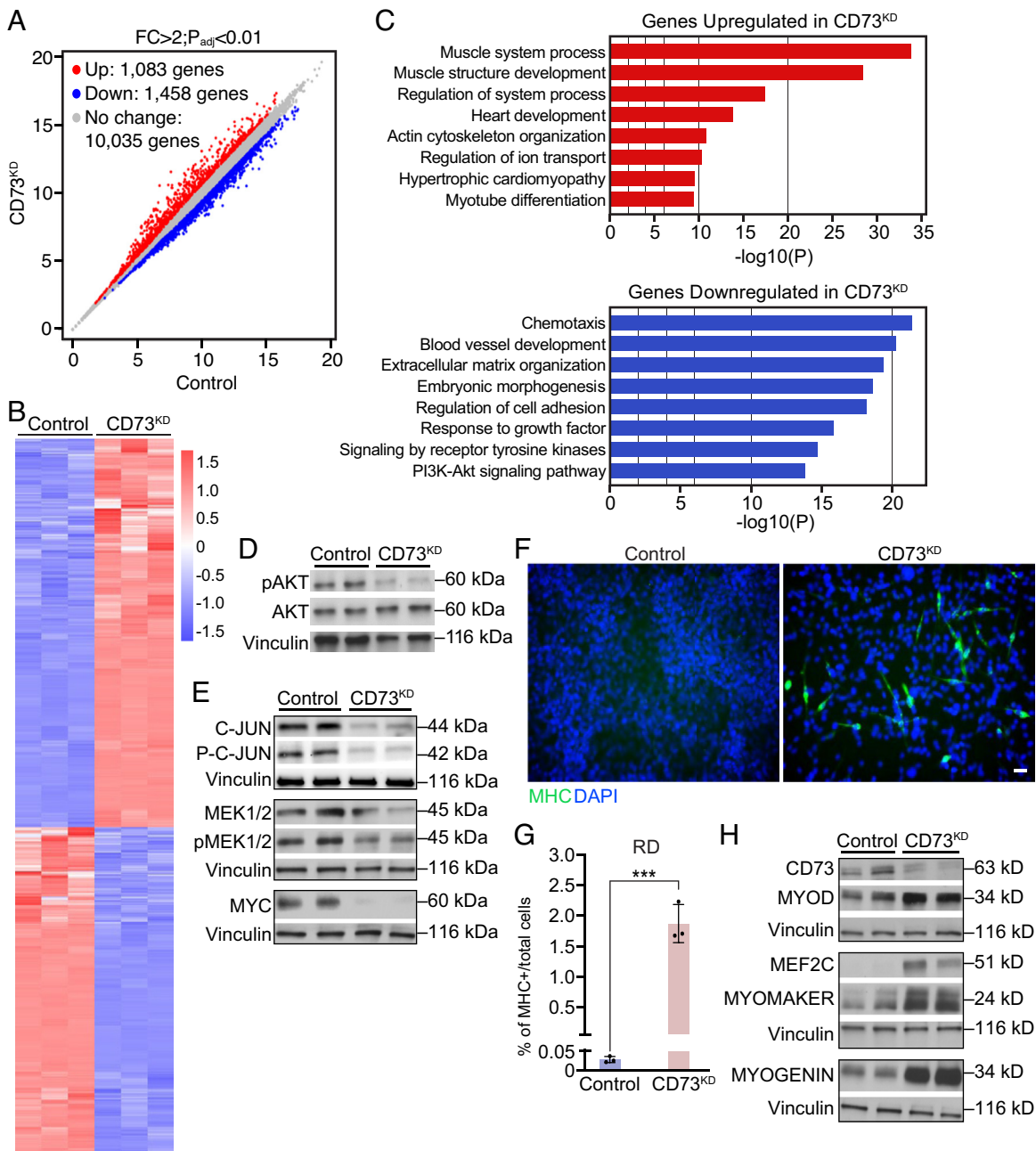


**Fig. 4.** CD73 knockdown induces myogenesis while decreasing oncogenic gene expression. (A) Volcano plot and (B) heat map showing log<sub>2</sub> fold change of genes upregulated (red) and downregulated (blue) in CD73<sup>KD</sup> RD cells compared to No-Dox ish-CD73 control RD cells. (C) Top enriched GO terms for differentially expressed genes in CD73<sup>KD</sup> RD cells compared to No-Dox ish-CD73 control RD cells. (D) Western blot analysis showing protein levels of AKT and pAKT in CD73<sup>KD</sup> RD cells compared to No-Dox ish-CD73 control RD cells. Vinculin is the control for total protein. (E) Western blot for C-JUN, P-C-JUN, MEK1/2, pMEK1/2, and MYC in CD73<sup>KD</sup> RD cells compared to No-Dox ish-CD73 control RD cells. Vinculin is the control for total protein. (F) Myogenic differentiation experiment in CD73<sup>KD</sup> RD cells subjected to differentiation media compared to No-Dox ish-CD73 control RD cells. After differentiation experiment, cells were stained with an antibody against Myosin Heavy Chain (MHC) (Green). Nuclei were stained with DAPI (blue). (Scale bar, 50 μm.) (G) Quantification of MHC-positive cells over the total number of cells in E; n = 3 independent experiments \*\*\*P < 0.001, results are shown as mean ± SEM; Student's *t* test two-tailed. (H) Western blot analysis for protein levels of CD73, MYOD, MEF2C, MYOMAKER, and MYOGENIN after 6 d of differentiation in CD73<sup>KD</sup> RD cells compared to No-Dox ish-CD73 control RD cells. Vinculin is the control for total protein.

#### Enzymatic Activity of CD73 Is Required for FN-RMS Pathogenesis.

We sought to investigate the mechanism by which CD73 contributes to the oncogenesis of FN-RMS. We hypothesized that the enzymatic activity of CD73 is responsible for its pathogenic role in this type of cancer. The residues Asp-85, His-118, and Arg-395 have been predicted to confer catalytic activity to CD73 (23). We mutated these three amino acid residues to alanine to generate a catalytically inactive CD73 mutant (Flag-3A-CD73). This construct lacked the two transmembrane domains of CD73 and included an N-terminal osteonectin signal sequence (ON) for extracellular

localization of the protein and a C-terminal 3X-flag for affinity purification (23). The control, Flag-WT-CD73, did not harbor the mutations (Fig. 5A). We overexpressed these constructs in Lenti-X 293T cells, collected the conditioned media, and purified the proteins (SI Appendix, Fig. S4A). Then, we tested the ability of the purified Flag-WT-CD73 and Flag-3A-CD73 proteins to hydrolyze AMP using the Malachite green assay to detect inorganic phosphate. While the Flag-WT-CD73 protein released inorganic phosphate when coincubated with AMP, the Flag-3A-CD73 mutant protein did not, confirming its lack of enzymatic activity (Fig. 5B).

Next, we performed gain of function experiments by overexpressing the full-length WT-CD73 (FL-WT-CD73) and full-length 3A-CD73 (FL-3A-CD73) constructs in RD cells and validating their overexpression by western blot analysis (*SI Appendix, Fig. S4B*). EdU staining showed no change in the proliferation of RD cells when either FL-WT-CD73 or FL-3A-CD73 were overexpressed (*SI Appendix, Fig. S4C*). We then investigated whether overexpression

of the FL-WT-CD73 and FL-3A-CD73 constructs could rescue the growth defect in CD73<sup>KD</sup> RD cells. First, we induced CD73 knock-down in ish-CD73 RD cells by Dox administration. We used Dox-treated ish-Scr RD cells as control. Next, we overexpressed GFP, FL-WT-CD73, or FL-3A-CD73, and confirmed their expression at the mRNA and protein levels in both CD73<sup>KD</sup> and control RD cells (Fig. 5C and *SI Appendix, Fig. S4 D and E*). We then evaluated the

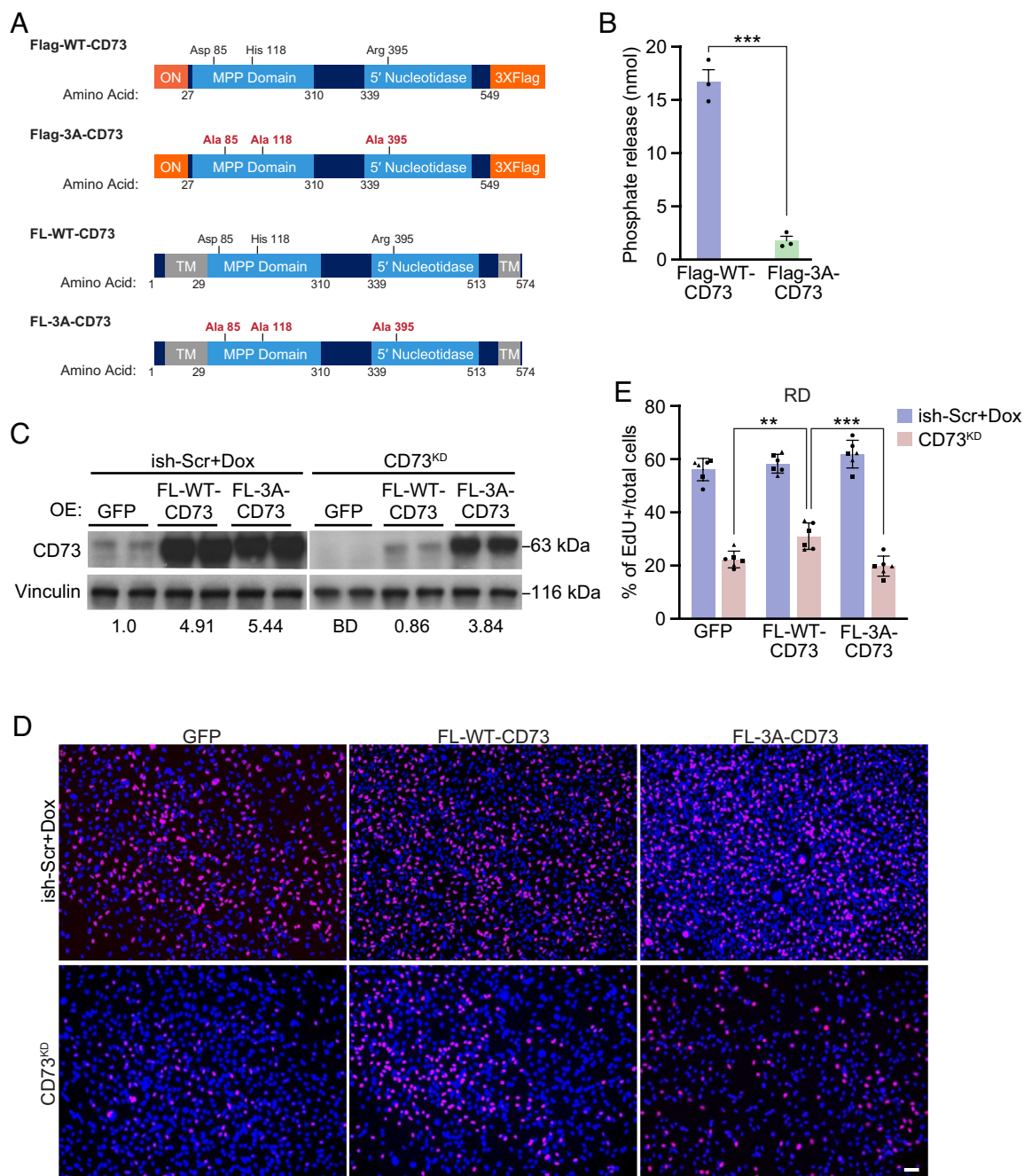


**Fig. 5.** The enzymatic activity of CD73 is required for FN-RMS cell growth. (A) Schematic of Flag-WT-CD73, Flag-3A-CD73, FL-CD73, and FL-3A-CD73 constructs. Flag-WT-CD73 and Flag-3A-CD73 were used for protein purification and malachite green assay. FL-WT-CD73 and FL-3A-CD73 were used for overexpression in RD cells. Transmembrane domain (TM), metallophosphatase domain (MPP), 5' nucleotidase, osteonectin signal sequence (ON), and 3XFlag tag (3XFlag). (B) Malachite green assay measuring phosphate release to examine the enzymatic activity of the purified Flag-3A-CD73 protein compared to Flag-WT-CD73;  $n = 3$  biologically independent experiments  $***P < 0.001$ , results are shown as mean  $\pm$  SEM; Student's  $t$  test two-tailed. (C) Western blot analysis in CD73<sup>KD</sup> RD cells compared to ish-Scr control RD cells (+Dox), infected with lentivirus containing FL-WT-CD73 and FL-3A-CD73 overexpression constructs. GFP was used as control for overexpression infection. Vinculin is the control for total protein. *Bottom:* Average densitometry ratios of FL-WT-CD73/GFP(ish-Scr+Dox) and FL-3A-CD73/GFP(ish-Scr+Dox). BD: below detection. (D) EdU staining (magenta) of CD73<sup>KD</sup> RD cells compared to ish-Scr control RD cells (+Dox), infected with FL-WT-CD73 and FL-3A-CD73 overexpression constructs. Nuclei were stained with DAPI (blue). GFP was used as control for overexpression. (Scale bar, 50  $\mu$ m.) (E) Quantification of EdU-positive cells over the total number of cells in D;  $n = 3$  independent experiments, duplicates in experiments are shown. CD73<sup>KD</sup> with GFP overexpression vs. CD73<sup>KD</sup> with FL-WT-CD73 overexpression  $**P < 0.01$ , CD73<sup>KD</sup> with FL-WT-CD73 overexpression vs. CD73<sup>KD</sup> with FL-3A-CD73 overexpression.  $***P < 0.001$ , results are shown as mean  $\pm$  SEM; two-way ANOVA.

effect of overexpressing these constructs on the proliferation of CD73<sup>KD</sup> and control ish-Scr RD cells. While there was no change in EdU incorporation in control ish-Scr RD cells (Fig. 5 *D* and *E*), we observed an increase in EdU incorporation when FL-WT-CD73 was overexpressed in CD73<sup>KD</sup> RD cells but not when FL-3A-CD73 mutant was overexpressed (Fig. 5 *D* and *E*). Overall, our findings show that the catalytic activity of CD73 is necessary for RD cell proliferation and may influence FN-RMS pathogenesis.

**CD73 Functions via the Purinergic Signaling Pathway to Maintain FN-RMS Growth.** Subsequently, we investigated whether CD73 promotes FN-RMS oncogenesis via the purinergic signaling pathway. In the extracellular space, the purinergic signaling pathway begins with CD39, which hydrolyzes ATP and ADP to AMP; then, AMP is further hydrolyzed to adenosine by CD73 (7). We hypothesized that knockdown of CD39, an upstream mediator of the pathway, would recapitulate the phenotype of CD73 knockdown in FN-RMS. To test this hypothesis, we treated RD cells for 48 h with a shRNA to knockdown CD39 (shCD39). The nontargeting scrambled shRNA (shScr) was used as control. We confirmed a reduction in CD39 mRNA levels by qRT-PCR in shCD39 relative to the shScr control (*SI Appendix, Fig. S5A*). EdU labeling experiments showed a substantial reduction in RD cell proliferation upon CD39 knockdown, similar to that observed upon CD73 knockdown in RD cells (Fig. 6 *A* and *B*).

After AMP is hydrolyzed to adenosine by CD73, adenosine can bind to adenosine receptors in the plasma membrane and initiate an intracellular cascade that stimulates cell proliferation (8). We investigated the effect of A<sub>2B</sub> adenosine receptor knockdown in RD cells using a shRNA (shA<sub>2B</sub>). After 48 h of shA<sub>2B</sub> treatment in RD cells, we confirmed A<sub>2B</sub> adenosine receptor knockdown by qRT-PCR relative to shScr (*SI Appendix, Fig. S5B*). Moreover, a decrease in EdU incorporation in RD cells upon A<sub>2B</sub> knockdown is reflective of its role in stimulating FN-RMS growth alongside CD39 and CD73 (Fig. 6 *C* and *D*). This finding led us to hypothesize that CD73 contributes to the pathogenesis of FN-RMS through the production of adenosine that results in the activation of the A<sub>2A-B</sub> adenosine receptors. To test this possibility, we treated CD73<sup>KD</sup> RD cells with the A<sub>2A-B</sub> adenosine receptor agonist CGS21680 for 48 h following CD73 knockdown. Exposure to the A<sub>2A-B</sub> adenosine receptor agonist (500 nM) was able to partially restore proliferation in the CD73<sup>KD</sup> RD cells (Fig. 6 *E* and *F*). As a control, we performed these experiments using the ish-Scr RD cells treated with Dox and did not observe any change in cell proliferation upon addition of the A<sub>2A-B</sub> agonist (*SI Appendix, Fig. S5C*), suggesting that the A<sub>2A-B</sub> agonist specifically overcomes the growth defect of CD73 knockdown. Additionally, we examined whether treatment with the A<sub>2A-B</sub> agonist could overcome the block to proliferation of JR-1 cells. We infected JR-1 cells with sh1-CD73 or shScr as control and then treated them with the A<sub>2A-B</sub> adenosine receptor agonist (500 nM) or DMSO for 48 h following CD73 knockdown. Similar to our rescue assays in RD cells, exposure to the A<sub>2A-B</sub> adenosine receptor agonist partially rescued the proliferation block resulting from CD73 knockdown in JR-1 cells (*SI Appendix, Fig. S5D* and *E*) and had no effect on the shScr-treated control cells (*SI Appendix, Fig. S5F*). Overall, these results suggest that CD73 maintains FN-RMS growth through its catalytic activity and subsequent adenosine-mediated A<sub>2A-B</sub> receptor activation (Fig. 6*G*).

## Discussion

CD73 plays a pivotal role in the purinergic signaling pathway through the hydrolysis of AMP to adenosine. Given the immunosuppressive nature of adenosine, the role of CD73 in suppressing

the immune system has been widely studied in many pathophysiological contexts, including cancer (9, 10). In addition, it has been suggested that CD73 can have immune-independent functions, which have been investigated to a much lesser extent (24, 25). In this study, we focused on the cell-autonomous role of CD73 in FN-RMS. We identified CD73 as a key protein contributing to the pathogenesis of FN-RMS and demonstrated that loss of CD73 activity results in reduced cell proliferation and tumor growth in vivo and diminished cell migration in vitro. Overactivation of AKT contributes to the malignant transformation and progression of multiple cancers, including RMS (8, 26, 27). We found that CD73 knockdown reduced the expression of genes related to the PI3K-AKT signaling pathway and decreased the phosphorylation of AKT in RD cells.

Hallmarks of RMS cells include an overproliferative state coupled with the lack of myogenic differentiation (1). Interestingly, CD73 is regulated by the TWIST2 transcription factor that has been previously shown to inhibit myogenesis (5). Therefore, we hypothesized that expression of CD73 maintains FN-RMS cells in a proliferative state leading to the inhibition of myogenic differentiation. Here, we found that knockdown of CD73 in FN-RMS cells, besides reducing cell growth, initiated the myogenic program and up-regulated the expression of terminal differentiation proteins. However, myogenic differentiation was observed only in a subset of cells. These results are consistent with other studies where only a small number of cells undergo terminal myogenic differentiation upon depletion of oncogenic factors (6, 28). In addition, a recent study showed that the RD cell line consists of a heterogeneous population of multiple cell states including proliferative, ground, and mesenchymal cell states (29). Therefore, we hypothesize that upon depletion of growth-promoting factors such as CD73, only cells that are further in the myogenic differentiation trajectory will undergo terminal myogenic differentiation, whereas cells in a primitive mesenchymal state will be resistant to differentiation.

Although it has been suggested that CD73 can exert enzymatic-dependent and -independent functions, the enzymatic activity of CD73 contributes to the pathogenesis of hepatocellular carcinoma and breast cancer (8, 30). Hence, we investigated whether the catalytic activity of CD73 is responsible for its role in FN-RMS growth by generating a catalytically inactive CD73 mutant. Through rescue experiments in cells with CD73 knockdown, we found that the catalytic activity of CD73 is necessary for FN-RMS pathogenesis. However, our rescue experiments did not show full recovery of proliferation upon FL-WT-CD73 overexpression. This could be due to potential nonenzymatic functions of CD73 in FN-RMS. Previously, it has been shown that CD73 contributes to breast cancer invasion and metastasis by regulating cell interactions with extracellular matrix components (31). Therefore, CD73 could also exert nonenzymatic roles. The potential nonenzymatic functions of CD73 in FN-RMS represent an interesting future issue.

Activation of A<sub>2B</sub> adenosine receptors plays a critical role in tumor development (10). In this study, we found that similar to CD73 knockdown, upon CD39 or A<sub>2B</sub> adenosine receptor knockdown, proliferation of FN-RMS cells was reduced. This implies that the purinergic signaling pathway contributes to the pathogenesis of FN-RMS. We used an A<sub>2A-B</sub> adenosine receptor agonist to treat CD73 knockdown cells and observed restoration of their proliferative phenotype. Moreover, activation of adenosine receptors can lead to activation of intracellular pathways such as the PI3K-AKT signaling pathway (8), which was down-regulated upon CD73 knockdown. Neither treatment with A<sub>2A-B</sub> adenosine receptor agonist nor overexpression of FL-WT-CD73 increased



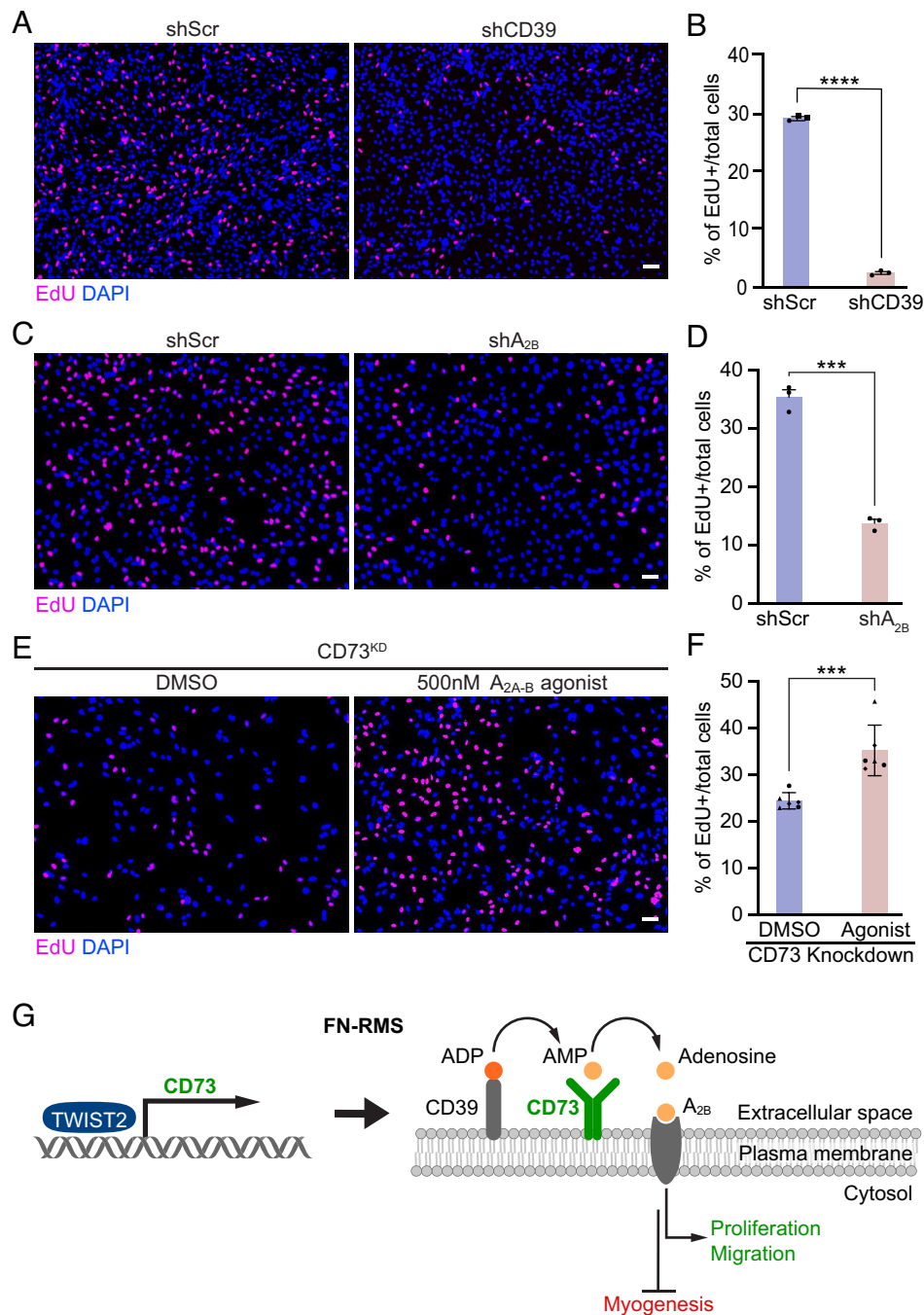


**Fig. 6.** CD73 contributes to FN-RMS through the purinergic signaling pathway. (A) EdU staining (magenta) of RD cells infected with shCD39 and shScr control. Nuclei were stained with DAPI (blue). (Scale bar, 50  $\mu\text{m}$ .) (B) Quantification of EdU-positive cells over total cells in A;  $n = 3$  biologically independent experiments \*\*\*\* $P < 0.001$ , results are shown as mean  $\pm$  SEM; Student's  $t$  test two-tailed. (C) EdU staining (magenta) of RD cells infected with shA<sub>2B</sub> and shScr control. Nuclei were stained with DAPI (blue). (Scale bar, 50  $\mu\text{m}$ .) (D) Quantification of EdU-positive cells over the total number of cells in C;  $n = 3$  biologically independent experiments \*\*\* $P < 0.001$ , results are shown as mean  $\pm$  SEM; Student's  $t$  test two-tailed. (E) EdU staining (magenta) of CD73<sup>KD</sup> RD cells treated with A<sub>2A-B</sub> agonist (CGS21680) compared to DMSO-treated CD73<sup>KD</sup> RD cells. Nuclei were stained with DAPI (blue). (Scale bar, 50  $\mu\text{m}$ .) (F) Quantification of EdU-positive cells over the total number of cells in E;  $n = 3$  biologically independent experiments, duplicates in experiments shown \*\*\* $P < 0.001$ , results are shown as mean  $\pm$  SEM; Student's  $t$  test two-tailed. (G) Proposed working model for the contribution of CD73 to the pathogenesis of FN-RMS.

proliferation in control cells. We speculate that these cancer cells are at the maximal proliferation capacity and a significant increase in proliferation is unlikely to occur.

Altogether, our results reveal that the catalytic activity of CD73 contributes to the pathogenic growth of FN-RMS through the activation of the purinergic signaling pathway. Inhibitors and neutralizing antibodies of CD73 and A<sub>2A-B</sub> adenosine receptors are in clinical trials and may warrant consideration for patients with FN-RMS (17–19, 32).

## Materials and Methods

**Proliferation assay.** A total of  $1.5 \times 10^5$  cells were seeded in a six-well plate. After treatment, the cells were pulsed with 10  $\mu\text{M}$  EdU (Lumiprobe-10540) for 2 h. Then, the cells were washed with PBS and fixed with 4% paraformaldehyde in PBS for 10 min at room temperature. Following fixation, the cells were permeabilized with 0.3% Triton X-100 in PBS for 10 min. Then, the cells were stained by adding the EdU master mix (8  $\mu\text{M}$  sulfo-Cy5-Azide, 2 mM CuSO<sub>4</sub>·5H<sub>2</sub>O, and 20 mg/mL Ascorbic acid in PBS) and incubating for 45 min. After EdU staining,

nuclei were counterstained with DAPI (Invitrogen, D1306, 1:2,000). The Keyence BZ-X700 microscope was used for imaging. Five pictures per well were taken, and analysis was made by calculating the average of cells with EdU+ nuclei over the total DAPI+ nuclei on the immunofluorescent staining images.

**Migration Assay.** Migration assay was performed using a transwell plate, according to the manufacturer's instructions (Corning-3422). A total of  $2 \times 10^5$  ish-CD73 RD cells were pretreated with or without Dox for 48 h before the assay. Untreated cells were used as control. Cells were seeded on top of the insert with 2% horse serum media, and 10% FBS media were placed in the bottom of the well. Migration was allowed to happen for 24 h. Then, the cells on the top of the insert were scraped followed by fixation and DAPI staining of the cells in the bottom of the insert, the ones that migrated. Images were taken using the Keyence Microscope.

**Differentiation and Immunofluorescence.** A total of  $1.5 \times 10^5$  ish-CD73 RD cells were seeded in a six-well plate with 2 mL of 10% TET system media. After 24 h, the cells were treated with or without 10 ng/mL of doxycycline for 48 h. Untreated cells were used as control. Then, the cells were washed with PBS and moved to differentiation media (DMEM with 2% horse serum and 100 U/mL penicillin/streptomycin) with the respective treatment. The cells were incubated for 5 d, and media were replenished every 48 h. After the treatment, the cells were fixed with 4% paraformaldehyde in PBS for 10 min and permeabilized with 0.5% Triton X-100 in PBS, followed by incubation with  $\alpha$ -myosin heavy chain (MyHC) (Sigma-M4276, 1:400, RRID:AB\_477190) in 2% goat serum in PBS overnight at 4 °C. The next day, the cells were incubated with Alexa 488 goat  $\alpha$ -mouse (Invitrogen-A-11001, 1:400, RRID:AB\_2534069) at room temperature for 1 h. Nuclei were counterstained with DAPI. Pictures were taken using the Keyence microscope. ImageJ was used to process the images, and quantification was done by counting the amount of MyHC<sup>+</sup> cells over the total number of nuclei.

**Xenograft Generation.** To generate xenograft models, NOD.Cg-Prkdc<sup>scid</sup> Il2rg<sup>tm1Wjl</sup>/SzJ (The Jackson Laboratory #005557, RRID: IMSR\_JAX:005557) mice were used. Eight mice were assigned per experimental group. The mice were kept in sterile conditions with a maximum of five mice per cage. The ish-CD73-luc RD cells were treated with or without 10 mg/mL doxycycline for 96 h. After treatment, the cells were collected, washed, and resuspended in PBS and then mixed 1:1 with Geltrex LDEV-Free Reduced Growth Factor Basement Membrane Matrix (Thermo Fisher Scientific A1413202). A total of  $7 \times 10^6$  cells were injected subcutaneously into the flank of a mouse. A caliper was used to measure the size of the tumor weekly followed by bioluminescent imaging (BLI) using IVIS (In Vivo Imaging System) Spectrum (PerkinElmer) in the AMI-HTX imager. For imaging, mice were anesthetized by controlled isoflurane through a nasal cone.

**Generation of the CD73 Constructs.** To test the enzymatic activity of CD73, two short CD73 mammalian expression plasmids were designed. First, amino acids 27-565 of the CD73 protein were fused to the N terminus of osteonectin (for extracellular localization) and to a C-terminal 3X-Flag tag for purification, as previously done (23). This served as the wild-type control (Flag-WT-CD73). The mutant, Flag-3A-CD73, had the same construct, but the predicted catalytic residues were mutated to Alanine. For the rescue experiment in cells, the FL-WT-CD73 and a FL-3A-CD73 mutant construct were used.

**CD73 Protein Purification.** Lenti-X 293T cells were transfected with the Flag-WT-CD73 and Flag-3A-CD73 plasmids with lentivirus packaging plasmids at a ratio of 3:1 using the FUGENE 6 transfection reagent, according to the manufacturer instructions. Viral media were used to generate stable Lenti-X 293T cell lines via infection and puromycin selection. These stable cell lines were used to secrete and generate the CD73-conditioned media. The conditioned media were collected every 2 d for 7 d (around 100 mL). The media were then incubated with 1 mL of 3X-Flag beads (From) at 4 °C overnight. The next day, the beads were washed with 25 mL of the wash buffer: 50 mM Tris-HCl (pH 7.5),

300 mM NaCl, 1 mM DTT, and 20 mM imidazole (pH 8), and eluted using 10 mL of elution buffer: 50 mM Tris-HCl (pH 7.5), 300 mM NaCl, 1 mM DTT, and 300 mM Imidazole (pH 8). The purified CD73 proteins were concentrated and stored at -80 °C until further use. The purity of the CD73 proteins was visualized and assessed via SDS-PAGE and Coomassie blue staining. Protein concentration was determined by Bradford assay.

**Malachite Green Assay.** The Malachite green reagent was made by dissolving 13.5 mg of malachite oxalate in 30 mL of milli Q H<sub>2</sub>O followed by the addition of 10 mL of 4.2% (w/v) ammonium molybdate in 4M HCl. This solution was rotated on a nutator at 4 °C for at least 45 min and then filtered before use. Two hundred microliter ATPase reactions were performed in 100 mM Tris-HCl (pH 7.5), 6 mM MgCl<sub>2</sub>, 20 mM KCl, and 1 mM ATP using 1  $\mu$ g of the CD73 proteins for 3 h at 37 °C. Reactions were stopped with 800  $\mu$ L of malachite green reagent followed by addition of 100  $\mu$ L of 34% (w/v) sodium citrate. Resulting solutions were measured for absorbance at 620 nm to monitor free phosphate release from ATP. Assays were performed in technical duplicates in three independent experiments.

**Rescue Experiments.** FL-WT-CD73 and FL-3A-CD73 overexpression: ish-CD73 and ish-Scr RD cells were treated with Dox for 48 h and then infected with lentivirus containing the overexpression constructs. The following day, media were changed, and cells were incubated for 72 h. Dox treatment was administered throughout the whole experiment. A<sub>2AB</sub> receptor agonist treatment: A<sub>2</sub>-selective adenosine receptor agonist CGS21680 (Millipore Sigma- C141-5MG) was used to treat the cells upon 48 h of Dox treatment at a concentration of 500 nM.

**Statistical Analysis.** Student's *t* test was used to analyze two comparative groups. For comparison analysis between multiple groups, the two-way ANOVA test was performed. All statistical analysis was performed using the GraphPad Prism 9 software. Values are expressed as mean  $\pm$  SEM. Values were considered statistically significant with *P* values (\**P* < 0.05, \*\**P* < 0.01, \*\*\**P* < 0.001, and \*\*\*\**P* < 0.0001).

**Data, Materials, and Software Availability.** Sequencing data generated in this study are deposited in the Gene Expression Omnibus dataset under accession number [GSE240722](https://www.ncbi.nlm.nih.gov/geo/query/acc.cgi?acc=GSE240722) (33).

**ACKNOWLEDGMENTS.** We thank Drs. Kathryn O'Donnell, Xurde Menendez Caravia, Stephanie Vargas Aguilar, Yichi Zhang, Mauricio Marquez-Palencia, and Gabriela Morales for helpful scientific discussions, J. Cabrera for graphics, Drs. S. Skapek's and R. Gallindo's laboratories for providing FN-RMS cell lines, Drs. J. Xu and Y. J. Kim from the Children's Research Institute Sequencing Facility for Illumina sequencing, R. Kittler and V. Schmid from the McDermott Center Next Generation Sequencing (NGS) Core and P. Raj and C. Liang from the Genomics Core facilities for NGS, Michael Story, Debabrata Saha, and Gabrielle Poeta from the UTSW Pre-Clinical Radiation Core Facility for AMI-HTX machine for luciferase imaging, J. Shelton from the Molecular Histopathology Core for assisting with tissue processing and H&E, and Michael Ortiz from Moody Foundation Flow Cytometry Facility for assistance with flow cytometry analysis. This work was supported by funds from Cancer Prevention & Research Institute of Texas RP2000103, the Robert A. Welch Foundation (Grant 1-0025 for E.N.O.), NIH-National Cancer Institute 5F31CA271675-02 (K.C.H.), and Hannah H. Gray Fellows Program Award (V.A.L.).

Author affiliations: <sup>a</sup>Department of Molecular Biology, University of Texas Southwestern Medical Center, Dallas, TX 75390; <sup>b</sup>Hamon Center for Regenerative Science and Medicine, University of Texas Southwestern Medical Center, Dallas, TX 75390; <sup>c</sup>Harold C. Simmons Comprehensive Cancer Center, University of Texas Southwestern Medical Center, Dallas, TX 75390; <sup>d</sup>HHMI, University of Texas Southwestern Medical Center, Dallas, TX 75390; and <sup>e</sup>Quantitative Biomedical Research Center, Peter O'Donnell Jr. School of Public Health, University of Texas Southwestern Medical Center, Dallas, TX 75390

1. S. X. Skapek et al., Rhabdomyosarcoma. *Nat. Rev. Dis. Primers* **5**, 1 (2019).
2. E. Missiaglia et al., PAX3/FOXO1 fusion gene status is the key prognostic molecular marker in rhabdomyosarcoma and significantly improves current risk stratification. *J. Clin. Oncol.* **30**, 1670-1677 (2012).
3. J. F. Shern et al., Comprehensive genomic analysis of rhabdomyosarcoma reveals a landscape of alterations affecting a common genetic axis in fusion-positive and fusion-negative tumors. *Cancer Discov.* **4**, 216-231 (2014).

4. D. S. Hawkins, S. L. Spunt, S. X. Skapek, C. O. G. S. T. S. Committee, Children's Oncology Group's 2013 blueprint for research: Soft tissue sarcomas. *Pediatr. Blood Cancer* **60**, 1001-1008 (2013).
5. S. Li et al., Twist2 amplification in rhabdomyosarcoma represses myogenesis and promotes oncogenesis by redirecting MyoD DNA binding. *Genes Dev.* **33**, 626-640 (2019).
6. A. M. Shah et al., TWIST2-mediated chromatin remodeling promotes fusion-negative rhabdomyosarcoma. *Sci. Adv.* **9**, eade8184 (2023).

7. T. Kordass, W. Osen, S. B. Eichmuller, Controlling the immune suppressor: Transcription factors and microRNAs regulating CD73/NT5E. *Front. Immunol.* **9**, 813 (2018).
8. X. L. Ma *et al.*, CD73 promotes hepatocellular carcinoma progression and metastasis via activating PI3K/AKT signaling by inducing Rap1-mediated membrane localization of P110beta and predicts poor prognosis. *J. Hematol. Oncol.* **12**, 37 (2019).
9. A. Young *et al.*, Co-inhibition of CD73 and A2AR adenosine signaling improves anti-tumor immune responses. *Cancer Cell* **30**, 391–403 (2016).
10. B. Allard, P. A. Beavis, P. K. Darcy, J. Stagg, Immunosuppressive activities of adenosine in cancer. *Curr. Opin. Pharmacol.* **29**, 7–16 (2016).
11. M. Roh, D. A. Wainwright, J. D. Wu, Y. Wan, B. Zhang, Targeting CD73 to augment cancer immunotherapy. *Curr. Opin. Pharmacol.* **53**, 66–76 (2020).
12. J. Zhu *et al.*, CD73/NT5E is a target of miR-30a-5p and plays an important role in the pathogenesis of non-small cell lung cancer. *Mol. Cancer* **16**, 34 (2017).
13. M. Turcotte *et al.*, CD73 promotes resistance to HER2/ErbB2 antibody therapy. *Cancer Res.* **77**, 5652–5663 (2017).
14. J. Stagg, E. Golden, E. Wennerberg, S. Demaria, The interplay between the DNA damage response and ectonucleotidases modulates tumor response to therapy. *Sci. Immunol.* **8**, eabq3015 (2023).
15. S. Burghoff *et al.*, Growth and metastasis of B16-F10 melanoma cells is not critically dependent on host CD73 expression in mice. *BMC Cancer* **14**, 898 (2014).
16. T. Jiang *et al.*, Comprehensive evaluation of NT5E/CD73 expression and its prognostic significance in distinct types of cancers. *BMC Cancer* **18**, 267 (2018).
17. B. Allard *et al.*, Anti-CD73 therapy impairs tumor angiogenesis. *Int. J. Cancer* **134**, 1466–1473 (2014).
18. B. Allard, M. Turcotte, J. Stagg, Targeting CD73 and downstream adenosine receptor signaling in triple-negative breast cancer. *Expert Opin. Ther. Targets* **18**, 863–881 (2014).
19. L. Buisseret *et al.*, Clinical significance of CD73 in triple-negative breast cancer: Multiplex analysis of a phase III clinical trial. *Ann. Oncol.* **29**, 1056–1062 (2018).
20. Z. Kurago *et al.*, Inhibitors of the CD73-adenosinergic checkpoint as promising combinatory agents for conventional and advanced cancer immunotherapy. *Front. Immunol.* **14**, 1212209 (2023).
21. X. Shi *et al.*, Research progress on the PI3K/AKT signaling pathway in gynecological cancer (Review). *Mol. Med. Rep.* **19**, 4529–4535 (2019).
22. F. Rascio *et al.*, The pathogenic role of PI3K/AKT pathway in cancer onset and drug resistance: An updated review. *Cancers (Basel)* **13**, 3949 (2021).
23. D. P. Heuts *et al.*, Crystal structure of a soluble form of human CD73 with ecto-5'-nucleotidase activity. *ChemBiochem* **13**, 2384–2391 (2012).
24. M. Lupia *et al.*, CD73 regulates stemness and epithelial-mesenchymal transition in ovarian cancer-initiating cells. *Stem Cell Rep.* **10**, 1412–1425 (2018).
25. J. Yu *et al.*, Extracellular 5'-nucleotidase (CD73) promotes human breast cancer cells growth through AKT/GSK-3beta/beta-catenin/cyclinD1 signaling pathway. *Int. J. Cancer* **142**, 959–967 (2018).
26. M. Kilic-Eren, T. Boylu, V. Tabor, Targeting PI3K/Akt represses Hypoxia inducible factor-1alpha activation and sensitizes Rhabdomyosarcoma and Ewing's sarcoma cells for apoptosis. *Cancer Cell Int.* **13**, 36 (2013).
27. J. Yang *et al.*, Targeting PI3K in cancer: Mechanisms and advances in clinical trials. *Mol. Cancer* **18**, 26 (2019).
28. R. Ciarpica *et al.*, Pharmacological inhibition of EZH2 as a promising differentiation therapy in embryonal RMS. *BMC Cancer* **14**, 139 (2014).
29. Y. Wei *et al.*, Single-cell analysis and functional characterization uncover the stem cell hierarchies and developmental origins of rhabdomyosarcoma. *Nat. Cancer* **3**, 961–975 (2022).
30. Z. W. Gao, K. Dong, H. Z. Zhang, The roles of CD73 in cancer. *Biomed Res. Int.* **2014**, 460654 (2014).
31. X. Zhi *et al.*, RNA interference of ecto-5'-nucleotidase (CD73) inhibits human breast cancer cell growth and invasion. *Clin. Exp. Metastasis* **24**, 439–448 (2007).
32. R. C. Augustin *et al.*, Next steps for clinical translation of adenosine pathway inhibition in cancer immunotherapy. *J. Immunother. Cancer* **10**, e004089 (2022).
33. K. C. Hernandez *et al.*, CD73 contributes to the pathogenesis of Fusion-Negative Rhabdomyosarcoma through the purinergic signaling pathway. Gene Expression Omnibus (GEO). <https://www.ncbi.nlm.nih.gov/geo/query/acc.cgi>. Deposited 11 August 2023.